

---

---

# Phase I Study of $^{99m}\text{Tc}$ -ADAPT6, a Scaffold Protein–Based Probe for Visualization of HER2 Expression in Breast Cancer

Olga Bragina<sup>1,2</sup>, Emma von Witting<sup>3</sup>, Javad Garousi<sup>4</sup>, Roman Zelchan<sup>1,2</sup>, Mattias Sandström<sup>5,6</sup>, Anna Orlova<sup>2,7</sup>, Anna Medvedeva<sup>1</sup>, Artem Doroshenko<sup>8</sup>, Anzhelika Vorobyeva<sup>2,4</sup>, Sarah Lindbo<sup>3</sup>, Jesper Borin<sup>3</sup>, Natalya Tarabanovskaya<sup>8</sup>, Jens Sörensen<sup>5</sup>, Sophia Hober<sup>3</sup>, Vladimir Chernov<sup>1,2</sup>, and Vladimir Tolmachev<sup>2,4</sup>

<sup>1</sup>Department of Nuclear Medicine, Cancer Research Institute, Tomsk National Research Medical Center, Russian Academy of Sciences, Tomsk, Russia; <sup>2</sup>Research Centrum for Oncotheranostics, Research School of Chemistry and Applied Biomedical Sciences, Tomsk Polytechnic University, Tomsk, Russia; <sup>3</sup>Department of Protein Science, School of Engineering Sciences in Chemistry, Biotechnology, and Health, KTH Royal Institute of Technology, Stockholm, Sweden; <sup>4</sup>Department of Immunology, Genetics, and Pathology, Uppsala University, Uppsala, Sweden; <sup>5</sup>Radiology and Nuclear Medicine, Department of Surgical Sciences, Uppsala University, Uppsala, Sweden; <sup>6</sup>Medical Physics, Uppsala University Hospital, Uppsala, Sweden; <sup>7</sup>Department of Medicinal Chemistry, Uppsala University, Uppsala, Sweden; and <sup>8</sup>Department of General Oncology, Cancer Research Institute, Tomsk National Research Medical Center, Russian Academy of Sciences, Tomsk, Russia

**Key Words:** HER2; ADAPT6;  $^{99m}\text{Tc}$ ; SPECT; phase I

**J Nucl Med 2021; 62:493–499**  
DOI: 10.2967/jnumed.120.248799

Radionuclide molecular imaging of human epidermal growth factor receptor type 2 (HER2) expression may help to stratify breast and gastroesophageal cancer patients for HER2-targeting therapies. Albumin-binding domain–derived affinity proteins (ADAPTs) are a new type of small (46–59 amino acids) protein useful as probes for molecular imaging. The aim of this first-in-humans study was to evaluate the biodistribution, dosimetry, and safety of the HER2-specific  $^{99m}\text{Tc}$ -ADAPT6. **Methods:** Twenty-nine patients with primary breast cancer were included. In 22 patients with HER2-positive ( $n = 11$ ) or HER2-negative ( $n = 11$ ) histopathology, an intravenous injection of  $385 \pm 125$  MBq of  $^{99m}\text{Tc}$ -ADAPT6 was performed, randomized to an injected protein mass of either 500  $\mu\text{g}$  ( $n = 11$ ) or 1,000  $\mu\text{g}$  ( $n = 11$ ). Planar scintigraphy followed by SPECT imaging was performed after 2, 4, 6, and 24 h. An additional cohort ( $n = 7$ ) was injected with  $165 \pm 29$  MBq (injected protein mass, 250  $\mu\text{g}$ ), and imaging was performed after 2 h only. **Results:** Injections of  $^{99m}\text{Tc}$ -ADAPT6 were well tolerated at all mass levels and not associated with adverse effects.  $^{99m}\text{Tc}$ -ADAPT6 cleared rapidly from the blood and most other tissues. The normal organs with the highest accumulation were the kidney, liver, and lung. Effective doses were  $0.009 \pm 0.002$  and  $0.010 \pm 0.003$  mSv/MBq for injected protein masses of 500 and 1,000  $\mu\text{g}$ , respectively. Injection of 500  $\mu\text{g}$  resulted in excellent discrimination between HER2-positive and HER2-negative tumors as early as 2 h after injection (tumor-to-contralateral breast ratio,  $37 \pm 19$  vs.  $5 \pm 2$ ;  $P < 0.01$ ). The tumor-to-contralateral breast ratios for HER2-positive tumors were significantly ( $P < 0.05$ ) higher for an injected mass of 500  $\mu\text{g}$  than for either 250 or 1,000  $\mu\text{g}$ . **Conclusion:** Injections of  $^{99m}\text{Tc}$ -ADAPT6 are safe and associated with low absorbed and effective doses. A protein dose of 500  $\mu\text{g}$  is preferable for discrimination between tumors with high and low expression of HER2. Further studies are justified to evaluate whether  $^{99m}\text{Tc}$ -ADAPT6 can be used as an imaging probe to stratify patients for HER2-targeting therapy in areas where PET imaging is not readily available.

**H**uman epidermal growth factor receptor type 2 (HER2) is a molecular target for several therapeutics for breast and gastroesophageal cancers. The response to such therapeutics depends on the HER2 expression level, and assessment of HER2 status in tumors is required to avoid under- and overtreatments (1,2). The current standard of care includes collecting biopsy material followed by an assessment of HER2 status using immunohistochemistry and in situ hybridization analysis. Tumors with a 3+ immunohistochemistry score or a 2+ score and positive for in situ hybridization are considered HER2-positive and eligible for HER2-targeting treatment. However, a major issue is HER2-expression heterogeneity, and breast cancer patients often have both HER2-positive and HER2-negative metastases (3,4). The invasiveness of biopsies prevents sampling of all metastases, which is associated with a risk of nonrepresentative findings.

Radionuclide molecular imaging of HER2 expression is a noninvasive approach to stratification, offering the advantage of repetitive mapping of HER2 expression in multiple metastases (5–7). One strategy is immuno-PET, which uses specific recognition of HER2 by monoclonal antibodies and the superior spatial resolution, registration efficiency, and quantification accuracy of PET. The therapeutic anti-HER2 antibodies trastuzumab (3,8–12) and pertuzumab (13), labeled with the long-lived positron emitters  $^{89}\text{Zr}$  or  $^{64}\text{Cu}$ , have been evaluated in patients. Clinical studies found potential for radionuclide molecular imaging of HER2. For example,  $^{89}\text{Zr}$ -trastuzumab PET imaging has resulted in altered therapeutic decisions for 40% of patients when clinically important lesions could not be biopsied (12). However, the use of full-length antibodies is complicated by slow penetration into tumors and slow clearance. This prolongs the time between injection and imaging, with the best results obtained 4–8 d after injection (8,13). Full-sized antibodies also accumulate in tumors unspecifically, creating a risk of false-positive diagnostics (11).

---

Received May 1, 2020; revision accepted Jul. 3, 2020.  
For correspondence or reprints contact: Vladimir Tolmachev, Department of Immunology, Genetics, and Pathology, Uppsala University, SE-75181, Uppsala, Sweden.  
E-mail: vladimir.tolmachev@igp.uu.se  
Published online Aug. 17, 2020.  
COPYRIGHT © 2021 by the Society of Nuclear Medicine and Molecular Imaging.

A possible alternative to immuno-PET is the use of much smaller targeting vectors, such as single-domain antibodies or engineered scaffold proteins (14). Both <sup>68</sup>Ga-labeled HER2-specific single-domain antibody (15) and Affibody molecules (Affibody AB) (4) have enabled high-contrast imaging of HER2-expressing breast cancer tumors and their metastases within 1.5–4 h after injection, showing that the use of scaffold proteins is a promising strategy for developing probes for radionuclide molecular imaging.

Albumin-binding domain–derived affinity proteins (ADAPTs) are derived from the 3-helical scaffold of the albumin-binding domain of streptococcal protein G (16). The small size of ADAPTs (46–59 amino acids; molecular weight, 5–7 kDa) and affinity in the low-nanomolar range create preconditions for their successful use as imaging agents. A series of ADAPTs was previously preclinically evaluated as HER2-imaging probes (17). To facilitate clearance of unbound agent from blood, an ADAPT variant, ADAPT6, that does not bind to albumin has been created

**TABLE 1**  
Patient Characteristics Before Injection with <sup>99m</sup>Tc-ADAPT6

Patient no	Age (y)	HER2 status of primary tumor	Primary tumor ER/PgR	Stage
500 µg; mean tumor size, 23 ± 8 mm				
1	36	3+ (IHC)	ER+/PgR-	IIB (T2N1M0)
2	63	3+ (IHC)	ER-/PgR-	IIIA (T3N1M0)
3	50	3+ (IHC)	ER+/PgR-	IIIA (T2N2M0)
4	61	3+ (IHC)	ER-/PgR-	IIB (T2N1M0)
5	64	2+ (IHC)/FISH+	ER-/PgR-	IIIB (T2N1M0)/IV (T2N3M1)*
6	34	0 (IHC)	ER+/PgR+	I (T1N0M0)
7	47	0 (IHC)	ER+;/PgR+	IIA (T2N0M0)
8	41	0 (IHC)	ER+/PgR+	IIA (T2N0M0)
9	63	1+ (IHC)	ER+/PgR+	IIB (T2N1M0)
10	59	1+ (IHC)	ER+/PgR-	IIA (T2N0M0)
11	40	0 (IHC)	ER-/PgR-	IIIA (T3N1M0)
1,000 µg; mean tumor size, 31 ± 11 mm				
12	34	3+ (IHC)	ER+/PgR-	IIA (T2N0M0)
13	37	3+ (IHC)	ER+/PgR-	IIA (T1N1M0)
14	43	2+ (IHC)/FISH+	ER+/PgR+	IIA (T2N0M0)
15	36	3+ (IHC)	ER+/PgR+	IIA (T1N1M0)
16	33	3+ (IHC)	ER-/PgR-	IIA (T2N0M0)
17	58	3+ (IHC)/2+ (IHC)/FISH <sup>†</sup>	ER+/PgR+	I (T1N0M0)
18	51	1+ (IHC)	ER+/PgR-	IIA (T2N0M0)
19	63	1+ (IHC)	ER+/PgR+	IIA (T2N0M0)
20	62	0 (IHC)	ER-/PgR-	IIA (T2N0M0)
21	71	1+ (IHC)	ER+/PgR-	IIA (T2N0M0)
22	42	0 (IHC)	ER+/PgR+	IIA (T2N0M0)
250 µg; mean tumor size, 30 ± 10 mm				
23	51	2+ (IHC)/FISH+	ER+/PgR-	IIA (T2N0M0)
24	48	2+ (IHC)/FISH+	ER+/PgR-	IIA (T2N0M0)
25	61	2+ (IHC)/FISH+	ER+/PgR+	IIA (T4N1M0)
26	39	3+ (IHC)	ER+/PgR-	IIA (T2N0M0)
27	29	2+ (IHC)/FISH-	ER+/PgR+	IIA (T2N0M0)
28	62	1+ (IHC)	ER+/PgR+	I (T1N0M0)
29	48	1+ (IHC)	ER-; PgR-	I (T1N0M0)

\*Staging was changed as imaging revealed distant metastases.

<sup>†</sup>FISH analysis after imaging confirmed HER2-negative status.

ER = estrogen receptor; IHC = immunohistochemistry; PgR = progesterone receptor.

(17). We have demonstrated that radiolabeled ADAPT6 is capable of specific high-contrast imaging of HER2-expressing human xenografts in mice a few hours after injection (18). Our studies suggested that labeling of hexahistidine-containing ADAPT6 using  $^{99m}\text{Tc}(\text{H}_2\text{O})_3(\text{CO})_3$  provides an agent with an affinity of 2.8 nM, which is suitable for imaging of HER2 using SPECT or planar  $\gamma$ -scintigraphy (19).

In this first-in-humans study (ClinicalTrials.gov identifier NCT03991260), we evaluated the distribution of  $^{99m}\text{Tc}$ -ADAPT6 in patients with primary HER2-positive and HER2-negative breast cancer. The primary objectives were to assess the distribution of  $^{99m}\text{Tc}$ -ADAPT6 in normal tissues and in tumors over time, to evaluate the dosimetry of  $^{99m}\text{Tc}$ -ADAPT6, and to obtain initial information on the safety and tolerability of  $^{99m}\text{Tc}$ -ADAPT6 after a single intravenous injection. The secondary objective was to compare the tumor imaging data with HER2 expression data obtained by immunohistochemistry and fluorescent in situ hybridization (FISH) analysis of biopsy samples.

Because the data for another scaffold protein, Affibody, demonstrated that an increase in the injected protein mass could increase the tumor-to-liver ratio and improve discrimination between tumors with high and low HER2 expression (4), we evaluated planar scintigraphy and SPECT imaging at 2, 4, 6, and 24 h after injection of 500 and 1,000  $\mu\text{g}$  of  $^{99m}\text{Tc}$ -ADAPT6. In addition, imaging at 2 h after injection of 250  $\mu\text{g}$  of  $^{99m}\text{Tc}$ -ADAPT6 was performed on a smaller cohort of patients.

## MATERIALS AND METHODS

### Patients

This was a prospective, open-label, nonrandomized phase I diagnostic study in patients with untreated primary breast cancer. The initial protocol and further extension of the patient cohort were approved by the Scientific Council of the Cancer Research Institute and Board of Medical Ethics, Tomsk National Research Medical Center of the Russian Academy of Sciences, and all subjects gave written informed consent. Female patients (18–80 y) with primary breast cancer were eligible. The inclusion criteria were a diagnosis of primary breast cancer with possible lymph node metastases; availability of HER2 status determined according to the guidelines of the American Society of Clinical Oncology (1); volumetrically quantifiable tumor lesions on CT, with at least 1 lesion larger than 1.0 cm in greatest diameter; hematologic, liver, and renal function test results within reference limits; a negative pregnancy test; and capability of undergoing the diagnostic investigations planned for the study. The exclusion criteria were a second, nonbreast, malignancy; autoimmune disease; active infection or history of severe infection; or administration of another investigational medicinal product. Twenty-nine patients were enrolled (Table 1; Fig. 1).

As a local standard of care, all patients underwent biopsy sampling; mammography (Giotto Image); bone scanning (Siemens e.cam 180) using  $^{99m}\text{Tc}$ -pyrophosphate; chest CT (Siemens Somatom Emotion 16 ECO); and ultrasound of the breast, regional lymph nodes, and liver (GE Healthcare Logiq E9). For patient 5, an additional MRI (Siemens Magnetom Essenza, 1.5-T) examination was performed.

The level of expression of HER2 in biopsy samples was determined by immunohistochemistry using HercepTest (Dako). In tumors with a score of 2+ or in cases of questionable results, HER2 amplification was assessed using FISH. The tumors were classified as HER2-positive (HercepTest score of 3+, or a score of 2+ and FISH-positive) or HER2-negative (HercepTest score of 0 or 1+, or a score of 2+ but FISH-negative).

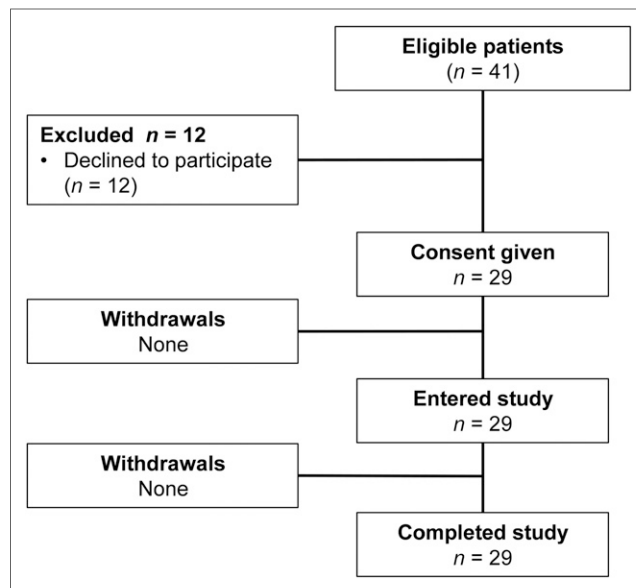


**FIGURE 1.** Flow diagram according to Standards for Reporting of Diagnostic Accuracy Studies (STARD).

### Imaging Protocol

ADAPT6 was labeled under aseptic conditions according to a method described earlier (19). The yield was  $77\% \pm 9\%$ , and radiochemical purity was  $99\% \pm 1\%$ .

$^{99m}\text{Tc}$ -ADAPT6 was injected as an intravenous bolus. Patients 1–11 were injected with 500  $\mu\text{g}$  of ADAPT6 ( $416 \pm 135$  MBq), and patients 12–22 were injected with 1,000  $\mu\text{g}$  ( $349 \pm 133$  MBq). Patients 23–29 were injected with 250  $\mu\text{g}$  ( $165 \pm 29$  MBq), and planar whole-body and SPECT scans were performed at 2 h. Imaging was performed using a scanner (e.cam 180) equipped with a high-resolution low-energy collimator and interfaced with a computer system for scintigraphic data processing (Siemens e.soft system). Anterior and posterior planar whole-body imaging (at a scan speed of 12 cm/min,  $1,024 \times 256$  pixel matrix) and SPECT (32 projections, 30 s each,  $128 \times 128$  pixel matrix) were performed at 2, 4, 6, and 24 h. The SPECT data were reconstructed iteratively with a gaussian filter, applying scatter correction.

Vital signs and possible side effects were monitored during the imaging study (0–24 h after injection) and for 3–7 d after injection. Blood and urine were analyzed at 5 and 14 d after injection.

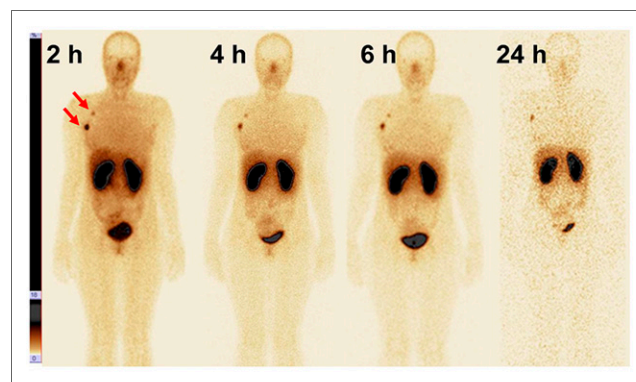


**FIGURE 2.** Anterior images at 2, 4, 6, and 24 h after injection of 500  $\mu\text{g}$  of  $^{99m}\text{Tc}$ -ADAPT6 (patient 1). Upper setting of scale window is 18% of maximum counts.

**TABLE 2**

Uptake of <sup>99m</sup>Tc in Tumor-Free Areas of Organs with Highest Uptake on SPECT Images After Injection of <sup>99m</sup>Tc-ADAPT6 (Decay-Corrected)

Time	Kidney			Lungs			Liver			Small intestine		
	250 µg	500 µg	1,000 µg	250 µg	500 µg	1,000 µg	250 µg	500 µg	1,000 µg	250 µg	500 µg	1,000 µg
2 h	26 ± 10	27 ± 10	35 ± 9	2.7 ± 0.9	3.3 ± 0.8	2.7 ± 0.6	3.1 ± 0.3	3.2 ± 1.1	2.4 ± 0.8	1.8 ± 0.4	0.8 ± 0.3	1.0 ± 0.3
4 h		31 ± 12	36 ± 10		2.5 ± 0.8	2.2 ± 0.4		2.8 ± 1.1	2.4 ± 1.0		0.9 ± 0.3	1.3 ± 0.5
6 h		32 ± 9	45 ± 11		2.0 ± 0.6*	2.0 ± 0.4*		2.6 ± 0.8	2.0 ± 0.7		0.8 ± 0.3†	1.3 ± 0.5
24 h		29 ± 10	38 ± 8		1.4 ± 0.5‡	1.2 ± 0.4‡		2.4 ± 1.0	1.8 ± 0.8		0.6 ± 0.2†	1.0 ± 0.3

\*Significantly ( $P < 0.05$ ) lower uptake in lungs at 6 h after injection than at 2 h.

†Significantly ( $P < 0.05$ ) lower uptake in intestinal content after injection of 500 µg than after 1,000 µg.

‡Significantly ( $P < 0.05$ ) lower uptake in lungs at 24 h after injection than at 2 or 4 h.

Data are percentage injected radioactivity per organ (mean values and SD from all patients).

**Assessment of Distribution and Dosimetry**

Regions of interest were drawn over organs of interest and the whole body on the anterior and posterior whole-body images of patients injected with 500 and 1,000 µg of <sup>99m</sup>Tc-ADAPT6; a geometric mean at 2, 4, 6, and 24 h was calculated for each region of interest. For quantification, a known activity of <sup>99m</sup>Tc in a water-filled phantom in combination with the Chang correction was used. To assess kinetics in blood, a region of interest was placed over the heart. Data were fitted by single exponential functions, and residence time was calculated as areas under fitted curves using Prism 8 (GraphPad Software, LLC). Absorbed doses were calculated by OLINDA/EXM 1.1 using the adult female phantom.

To calculate the tumor-to-contralateral breast and tumor-to-liver ratios, a 3.5-cm<sup>3</sup> volume of interest was drawn on tomograms centered on the highest tumor uptake, and counts were recorded. Thereafter, this volume of interest was copied to the contralateral breast and liver to obtain reference counts. The tumor-to-contralateral breast ratio for each primary tumor was calculated and matched with the biopsy-based data concerning HER2 expression in the tumor.

**Statistics**

Values are reported as mean ± SD. The significance of differences in organ uptake between different time points was analyzed using 1-way ANOVA. The significance of differences between tumor-to-contralateral breast and tumor-to-liver ratios for HER2-positive and HER2-negative tumors was analyzed using the nonparametric Mann-Whitney *U* test. A 2-sided *P* value of less than 0.05 was considered significant.

**RESULTS**

**Safety and Tolerability**

<sup>99m</sup>Tc-ADAPT6 was administered to 29 patients and was well tolerated. No drug-related adverse reactions or changes in vital signs were observed during imaging or the follow-up period. No changes were detected on blood or urine analysis.

**Distribution and Dosimetry**

The highest uptake in normal organs was in the kidneys, liver, and lungs (Fig. 2; Table 2). Moderate activity was observed in the gastrointestinal tract. Uptake in the salivary and lacrimal glands was also visualized. The activity distribution was similar after injection of 500 µg and 1,000 µg. The only significant difference ( $P < 0.05$ ) was in intestinal-content uptake at 6 and 24 h after injection, being lower for 500 µg. The decay-corrected uptake in

the kidneys, liver, lungs, and intestinal content plateaued by 2 h after injection.

The blood kinetics of <sup>99m</sup>Tc-ADAPT6 is shown in Figure 3. The elimination rates for 500 µg (half-life, 3.1 h; 95% CI, 2.4–4.0 h) and 1,000 µg (half-life, 3.0 h; 95% CI, 2.3–3.9 h) were similar.

Estimated absorbed doses are presented in Table 3. The highest was in the kidney. The doses to the adrenals, gallbladder wall, liver, spleen, and pancreas were also noticeable, but they were severalfold lower than the renal dose. The doses to the adrenals, stomach wall, spleen, thyroid, and uterus were significantly ( $P < 0.05$ ) higher for 1,000 µg, but the absolute difference was prominent only for the adrenal and thyroid. The total effective dose was  $0.009 \pm 0.002$  mSv/MBq for 500 µg and  $0.010 \pm 0.003$  mSv/MBq for 1,000 µg. For a typical injected activity in this study, 380 MBq, these total effective doses would result in an effective dose of 3.4 and 3.8 mSv, respectively.

**Discrimination Between Tumors with High and Low HER2 Expression**

All tumors (including 8 multicentric) and involved lymph nodes ( $n = 9$ ) with both high and low HER2 expression were visualized

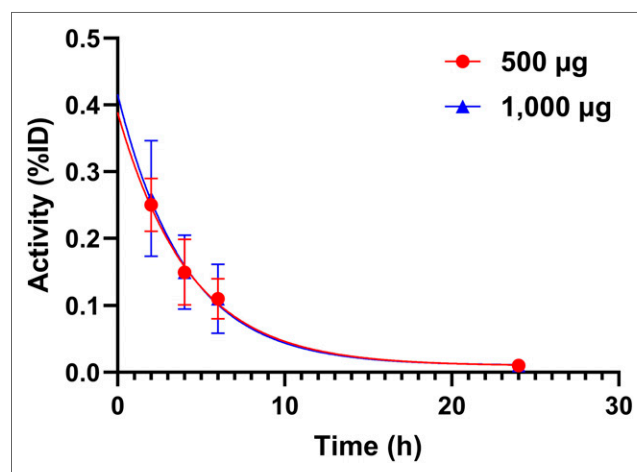


**FIGURE 3.** Kinetics of elimination of <sup>99m</sup>Tc-ADAPT6 from blood. Data are based on count rates in regions of interest placed over hearts. %ID = percentage injected dose.

**TABLE 3**  
Absorbed Doses After Injection of 500 and 1000  $\mu\text{g}$  of  $^{99\text{m}}\text{Tc}$ -ADAPT6

Site	500 $\mu\text{g}$	1,000 $\mu\text{g}$
Adrenals	0.023 $\pm$ 0.005*	0.032 $\pm$ 0.009
Brain	0.001 $\pm$ 0.000	0.001 $\pm$ 0.000
Breasts	0.007 $\pm$ 0.002	0.009 $\pm$ 0.005
Gallbladder wall	0.013 $\pm$ 0.008	0.012 $\pm$ 0.003
Lower large intestine wall	0.005 $\pm$ 0.001	0.005 $\pm$ 0.001
Small intestine	0.006 $\pm$ 0.001	0.008 $\pm$ 0.002
Stomach wall	0.006 $\pm$ 0.001*	0.008 $\pm$ 0.002
Upper large intestine wall	0.007 $\pm$ 0.001	0.008 $\pm$ 0.002
Heart wall	0.004 $\pm$ 0.001	0.004 $\pm$ 0.001
Kidney	0.135 $\pm$ 0.042	0.191 $\pm$ 0.047
Liver	0.011 $\pm$ 0.008	0.008 $\pm$ 0.002
Lungs	0.005 $\pm$ 0.001	0.006 $\pm$ 0.001
Muscle	0.003 $\pm$ 0.000	0.003 $\pm$ 0.001
Ovaries	0.008 $\pm$ 0.002	0.010 $\pm$ 0.003
Pancreas	0.011 $\pm$ 0.002	0.014 $\pm$ 0.004
Red marrow	0.004 $\pm$ 0.001	0.005 $\pm$ 0.001
Osteogenic cells	0.006 $\pm$ 0.001	0.008 $\pm$ 0.002
Skin	0.001 $\pm$ 0.000	0.002 $\pm$ 0.000
Spleen	0.011 $\pm$ 0.003*	0.015 $\pm$ 0.004
Thymus	0.005 $\pm$ 0.002	0.006 $\pm$ 0.002
Thyroid	0.009 $\pm$ 0.004*	0.014 $\pm$ 0.005
Urinary bladder wall	0.012 $\pm$ 0.007	0.012 $\pm$ 0.006
Uterus	0.005 $\pm$ 0.001*	0.007 $\pm$ 0.002
Total body	0.004 $\pm$ 0.001	0.005 $\pm$ 0.001
Effective dose equivalent (mSv/MBq)	0.017 $\pm$ 0.004	0.022 $\pm$ 0.005
Effective dose (mSv/MBq)	0.009 $\pm$ 0.002	0.010 $\pm$ 0.003

\*Significant ( $P < 0.05$ ) difference between doses after injection of 500 and 1,000  $\mu\text{g}$ .

Data are mean mGy/MBq  $\pm$  SD ( $n = 11$ ).

using  $^{99\text{m}}\text{Tc}$ -ADAPT6 as early as 2 h after injection and remained visible throughout the study (Figs. 2 and 4). Several visualized tumors were in agreement with the data from other radiology

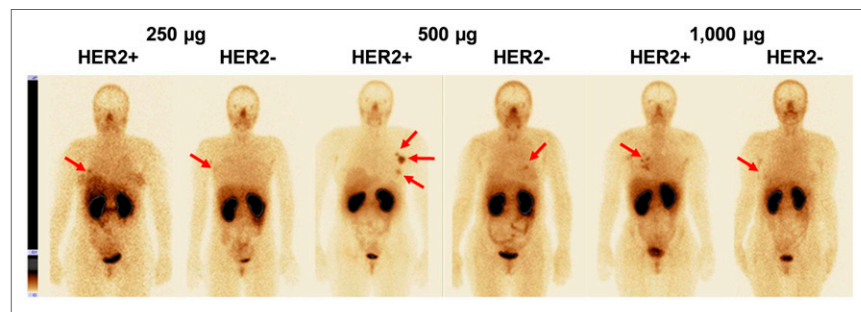


**FIGURE 4.** Representative anterior images of patients with HER2-negative and HER2-positive tumors (arrows) after injection of 250, 500, or 1,000  $\mu\text{g}$  of  $^{99\text{m}}\text{Tc}$ -ADAPT6. Upper setting of scale window is same for all images, 18% of maximum count rate.

investigations. Lymph node involvement was confirmed by histologic analysis after core biopsy ( $n = 3$ ) or cytologic analysis after fine-needle biopsy ( $n = 6$ ) with subsequent histologic analysis of surgical material.

The relationship between data concerning expression of HER2 in biopsy samples and tumor-to-contralateral breast ratios is presented in Figure 5 and Supplemental Figure 1 (supplemental materials are available at <http://jnm.snmjournals.org>). The best discrimination between tumors with high and low HER2 expression was provided by injection of 500  $\mu\text{g}$  of protein, for which the mean tumor-to-contralateral breast ratio for HER2-positive tumors was already  $37 \pm 19$  at 2 h after injection, significantly higher ( $P < 0.001$ , Mann-Whitney test) than for HER2-negative tumors ( $5 \pm 2$ ) (Fig. 5). The ratio tended to increase over time and was significantly ( $P < 0.05$ ) higher for 500  $\mu\text{g}$  than for 1,000  $\mu\text{g}$ . The difference in ratio between HER2-positive and HER2-negative tumors for 1,000  $\mu\text{g}$  was not significant ( $P > 0.05$ , Mann-Whitney test) at any time point (Fig. 5). The ratio for 250  $\mu\text{g}$  at 2 h ( $6.5 \pm 4.9$ ) was also significantly ( $P < 0.05$ ) lower than that for 500  $\mu\text{g}$  (Fig. 5).

Patient 17 was enrolled in this study because the initial immunohistochemistry evaluation of her biopsy samples suggested a 3+ expression level. However, her image showed an unusually low tumor-to-contralateral breast ratio (1.33 at 2 h). The biopsy samples were reevaluated by pathologists, and the HER2 status was reassigned as 2+ and FISH-negative. On the basis of the new pathologic evaluation, her HER2-targeting therapy was cancelled.

Imaging of patient 5 revealed, besides the primary tumor and axillary metastases, suspected bone metastases in rib 5 and vertebrae T8 and T9 (Fig. 6A). CT imaging and bone scanning using  $^{99\text{m}}\text{Tc}$ -pyrophosphate (Fig. 6B; Supplemental Figs. 2A and 2B) did not reveal any metastases. However, MRI confirmed metastases in T8 and T9 (Supplemental Fig. 3). The treatment strategy was changed from surgery to chemotherapy and HER2-targeting therapy.  $^{99\text{m}}\text{Tc}$ -pyrophosphate bone and CT scans (Fig. 6C; Supplemental Figs. 2C and 2D) confirmed metastatic lesions in rib 5 and in the T8 and T9 vertebrae 6 mo after  $^{99\text{m}}\text{Tc}$ -ADAPT6 imaging.

Injection of 500 or 1,000  $\mu\text{g}$  of  $^{99\text{m}}\text{Tc}$ -ADAPT6 enabled higher uptake in tumors than in liver (Fig. 7). There was a tendency toward higher tumor-to-liver ratios for the 500- $\mu\text{g}$  protein dose, but the difference between the ratios for the 500- and 1,000- $\mu\text{g}$  doses was not significant. Injection of 250  $\mu\text{g}$  resulted in significantly lower tumor-to-liver ratios than injection of 500  $\mu\text{g}$ .

## DISCUSSION

This study demonstrated that injections of  $^{99\text{m}}\text{Tc}$ -ADAPT6 are safe and well tolerated. The mean effective dose, 0.010 mSv/MBq, in this study corresponds to 3.8 mSv per patient, slightly lower than doses for imaging using  $^{68}\text{Ga}$ -ABY25 Affibody molecule (5.6 mSv) (20) or  $^{68}\text{Ga}$ -single-domain antibody (4.6 mSv) (15) and appreciably lower than effective doses for  $^{89}\text{Zr}$ -trastuzumab (18–38 mSv) (8,10) or  $^{89}\text{Zr}$ -pertuzumab (39 mSv) (13). Clear discrimination between HER2-positive and -negative tumors as early as 2 h after injection might permit a further 2-fold reduction of injection activity while preserving good imaging quality.



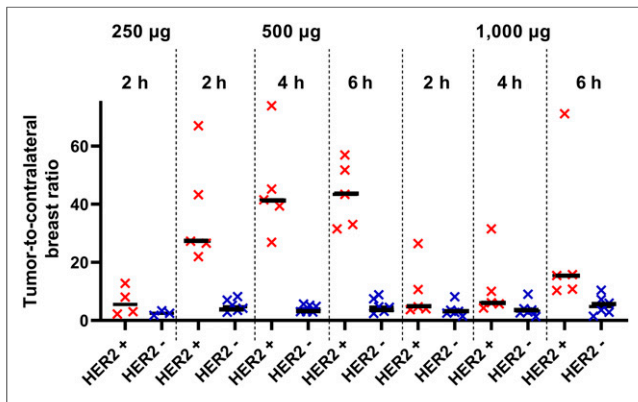


**FIGURE 5.** Primary tumor-to-contralateral breast ratio at 2 h after injection of 250 µg of  $^{99m}\text{Tc}$ -ADAPT6 and at 2, 4, and 6 h after injection of 500 and 1,000 µg. Red symbols represent data for HER2-positive tumors; blue, for HER2-negative.

Discrimination between HER2-positive and -negative lesions, helping to identify patients potentially responding to HER2-targeting therapy, is a primary aim of molecular imaging. However, the term *HER2-negative*, that is, unsuitable for treatment with HER2-targeting therapies, is deceptive. Breast tumors with an immunohistochemistry score of 2+ (and in situ hybridization-negative) are considered HER2-negative but may express up to 500,000 HER2 molecules per cell (21). Thus, some accumulation of imaging probes is expected even in HER2-negative lesions. Studies with anti-HER2 Affibody molecules demonstrated that it is possible to improve discrimination between tumors with high and low expression by increasing the injected protein mass (4,22). Furthermore, clinical data have shown that increasing the injected mass of  $^{68}\text{Ga}$ -labeled anti-HER2 Affibody molecules from 100 to 500 µg reduces binding to hepatocytes, which express low levels of HER2, and improves imaging of hepatic metastases (4). Studies on mice demonstrated that an increase in the injected dose of  $^{68}\text{Ga}$ -labeled ADAPT6 from 1 to 15 µg improved discrimination between human xenografts with high and low HER2 expression (18). However, an upscaling from mice to humans is quite uncertain. Therefore, we initially evaluated injection of  $^{99m}\text{Tc}$ -ADAPT6 at 2 dose levels, 500 and 1,000 µg. Injection of 500 µg provided excellent discrimination as early as 2 h after injection (Fig. 5), and the tumor-to-contralateral breast ratio

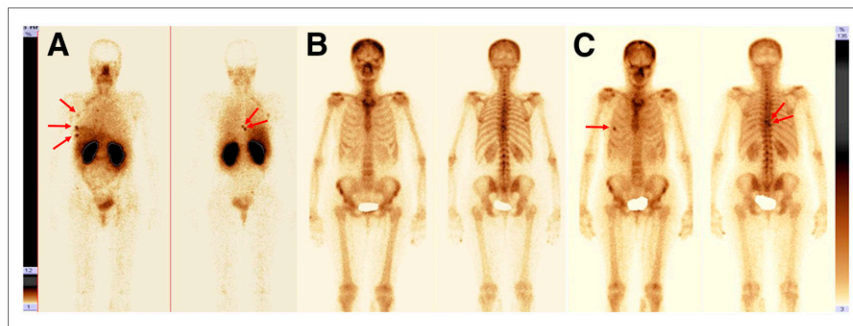


**FIGURE 6.** Tumor site visualization (arrows) with planar scintigraphy in patient 5 using  $^{99m}\text{Tc}$ -ADAPT6 at 2 h after injection (upper setting of scale window is 12% of maximum counts) (A);  $^{99m}\text{Tc}$ -pyrophosphate at time of imaging with  $^{99m}\text{Tc}$ -ADAPT6 (B); and  $^{99m}\text{Tc}$ -pyrophosphate 6 mo after ADAPT6 injection (C).

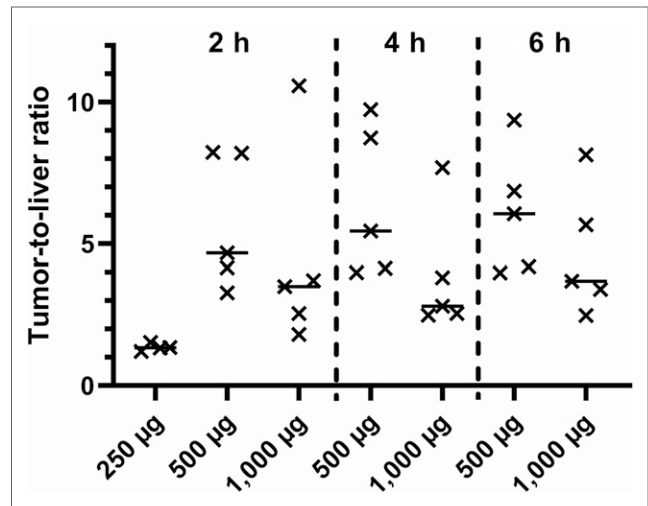


**FIGURE 7.** Tumor-to-liver ratio for HER2-positive tumors at 2 h after injection of 250 µg of  $^{99m}\text{Tc}$ -ADAPT6 and at 2, 4, and 6 h after injection of 500 and 1,000 µg.

had a tendency to increase over time. In contrast, injection of 1,000 µg did not enable discrimination between HER2-positive and -negative tumors. To check whether a further reduction of the injected protein mass would improve discrimination, an additional smaller cohort of patients was injected with 250 µg of  $^{99m}\text{Tc}$ -ADAPT6. However, the contrast of such imaging was clearly inferior to that of imaging using 500 µg (Fig. 5). Thus, a 500-µg dose appears optimal, and deviation from this dose would decrease both the sensitivity and the specificity of imaging of HER2 expression (Supplemental Fig. 4). Most likely, such a dose provides a delicate balance between saturation of HER2 in the liver, which increases the bioavailability of radiolabeled ADAPT6, and saturation of HER2 in tumors, which decreases  $^{99m}\text{Tc}$ -ADAPT6 uptake in HER2-positive lesions. The ability to perform early imaging enables reduction of the injected activity and, accordingly, of the effective dose to patients. Obviously, clinical imaging using  $^{99m}\text{Tc}$ -ADAPT6 should be performed approximately 2 h after injection. Increasing the interval between injection and imaging would require either increasing the injected activity (and consequently the effective dose) or decreasing the counting statistics at the time of imaging (and consequently the reconstruction fidelity).

PET provides better resolution, sensitivity, and quantification than SPECT but is costlier and requires substantially more infrastructure. Modern PET/CT facilities are installed mainly in Europe and North America, whereas SPECT is the most common nuclear imaging modality in Asia, Africa, and South America. SPECT imaging might also be of interest in other regions where PET is available but much more expensive or of restricted accessibility. It is conceivable that  $^{99m}\text{Tc}$ -labeled targeting proteins and peptides will be useful in these regions (23).

## CONCLUSION

$^{99m}\text{Tc}$ -ADAPT6 is safe and well tolerated. Injections of  $^{99m}\text{Tc}$ -ADAPT6 are

associated with low absorbed and effective doses. Among the injected protein doses tested, 500 µg provides the best discrimination between primary tumors with high expression of HER2 and primary tumors with low expression. Further studies on the use of <sup>99m</sup>Tc-ADAPT6 to stratify patients for HER2-targeted therapy are justified.

## DISCLOSURE

This research was financially supported by the Ministry of Science and Higher Education of the Russian Federation (grant 075-15-2019-1925). No other potential conflict of interest relevant to this article was reported.

## KEY POINTS

**QUESTION:** Is imaging of HER2 using <sup>99m</sup>Tc-ADAPT6 safe and informative?

**PERTINENT FINDINGS:** Imaging using <sup>99m</sup>Tc-ADAPT6 was safe and well tolerated. An injected protein dose of 500 µg provided discrimination between HER2-positive and HER2-negative primary breast tumors 2 h after injection.

**IMPLICATIONS FOR PATIENT CARE:** Data from this first-in-humans study support further clinical evaluation of <sup>99m</sup>Tc-ADAPT6 and, potentially, development of a probe for imaging of HER2 expression in regions where PET is not readily available.

## REFERENCES

1. Wolff AC, Hammond ME, Hicks DG, et al. Recommendations for human epidermal growth factor receptor 2 testing in breast cancer: American Society of Clinical Oncology/College of American Pathologists clinical practice guideline update. *J Clin Oncol*. 2013;31:3997–4013.
2. Bartley AN, Washington MK, Colasacco C, et al. HER2 testing and clinical decision making in gastroesophageal adenocarcinoma: guideline from the College of American Pathologists, American Society for Clinical Pathology, and the American Society of Clinical Oncology. *J Clin Oncol*. 2017;35:446–464.
3. Gebhart G, Lamberts LE, Wimana Z, et al. Molecular imaging as a tool to investigate heterogeneity of advanced HER2-positive breast cancer and to predict patient outcome under trastuzumab emtansine (T-DM1): the ZEPHIR trial. *Ann Oncol*. 2016;27:619–624.
4. Sörensen J, Velikyan I, Sandberg D, et al. Measuring HER2-receptor expression in metastatic breast cancer using [<sup>68</sup>Ga]ABY-025 Affibody PET/CT. *Theranostics*. 2016;6:262–271.
5. Tolmachev V. Imaging of HER-2 overexpression in tumors for guiding therapy. *Curr Pharm Des*. 2008;14:2999–3019.
6. Gebhart G, Flamen P, De Vries EG, Jhaveri K, Wimana Z. Imaging diagnostic and therapeutic targets: human epidermal growth factor receptor 2. *J Nucl Med*. 2016;57(suppl 1):81S–88S.
7. Mankoff DA, Edmonds CE, Farwell MD, Pryma DA. Development of companion diagnostics. *Semin Nucl Med*. 2016;46:47–56.
8. Dijkers EC, Oude Munnink TH, Kosterink JG, et al. Biodistribution of <sup>89</sup>Zr-trastuzumab and PET imaging of HER2-positive lesions in patients with metastatic breast cancer. *Clin Pharmacol Ther*. 2010;87:586–592.
9. Mortimer JE, Bading JR, Colcher DM, et al. Functional imaging of human epidermal growth factor receptor 2-positive metastatic breast cancer using <sup>64</sup>Cu-DOTA-trastuzumab PET. *J Nucl Med*. 2014;55:23–29.
10. Laforest R, Lapi SE, Oyama R, et al. [<sup>89</sup>Zr]trastuzumab: evaluation of radiation dosimetry, safety, and optimal imaging parameters in women with HER2-positive breast cancer. *Mol Imaging Biol*. 2016;18:952–959.
11. Ulaner GA, Hyman DM, Lyashchenko SK, Lewis JS, Carrasquillo JA. <sup>89</sup>Zr-trastuzumab PET/CT for detection of human epidermal growth factor receptor 2-positive metastases in patients with human epidermal growth factor receptor 2-negative primary breast cancer. *Clin Nucl Med*. 2017;42:912–917.
12. Bensch F, Brouwers AH, Lub-de Hooge MN, et al. <sup>89</sup>Zr-trastuzumab PET supports clinical decision making in breast cancer patients, when HER2 status cannot be determined by standard work up. *Eur J Nucl Med Mol Imaging*. 2018;45:2300–2306.
13. Ulaner GA, Lyashchenko SK, Riedl C, et al. First-in-human human epidermal growth factor receptor 2-targeted imaging using <sup>89</sup>Zr-pertuzumab PET/CT: dosimetry and clinical application in patients with breast cancer. *J Nucl Med*. 2018;59:900–906.
14. Krasniqi A, D'Huyvetter M, Devoogdt N, et al. Same-day imaging using small proteins: clinical experience and translational prospects in oncology. *J Nucl Med*. 2018;59:885–891.
15. Keyaerts M, Xavier C, Heemskerk J, et al. T. Phase I study of <sup>68</sup>Ga-HER2-nanobody for PET/CT assessment of HER2 expression in breast carcinoma. *J Nucl Med*. 2016;57:27–33.
16. Nilvebrant J, Hober S. The albumin-binding domain as a scaffold for protein engineering. *Comput Struct Biotechnol J*. 2013;6:e201303009.
17. Nilvebrant J, Åstrand M, Georgieva-Kotseva M, Björmalm M, Löfblom J, Hober S. Engineering of bispecific affinity proteins with high affinity for ERBB2 and adaptable binding to albumin. *PLoS One*. 2014;9:e103094.
18. Garousi J, Lindbo S, Nilvebrant J, et al. ADAPT, a novel scaffold protein-based probe for radionuclide imaging of molecular targets that are expressed in disseminated cancers. *Cancer Res*. 2015;75:4364–4371.
19. Lindbo S, Garousi J, Åstrand M, et al. Influence of histidine-containing tags on the biodistribution of ADAPT scaffold proteins. *Bioconjug Chem*. 2016;27:716–726.
20. Sandström M, Lindskog K, Velikyan I, et al. Biodistribution and radiation dosimetry of the anti-HER2 Affibody molecule <sup>68</sup>Ga-ABY-025 in breast cancer patients. *J Nucl Med*. 2016;57:867–871.
21. Ross JS, Fletcher JA, Bloom KJ, et al. Targeted therapy in breast cancer: the HER-2/neu gene and protein. *Mol Cell Proteomics*. 2004;3:379–398.
22. Tolmachev V, Wällberg H, Sandström M, Hansson M, Wennborg A, Orlova A. Optimal specific radioactivity of anti-HER2 Affibody molecules enables discrimination between xenografts with high and low HER2 expression levels. *Eur J Nucl Med Mol Imaging*. 2011;38:531–539.
23. Briganti V, Cuccurullo V, Di Stasio GD, Mansi L. Gamma emitters in pancreatic endocrine tumors imaging in the PET era: is there a clinical space for <sup>99m</sup>Tc-peptides? *Curr Radiopharm*. 2019;12:156–170.